T5 Inverse problems in biphasic millifluidic flow

J.C. Batsale[1], M. Romano[1], C. Pradere[1]
[1] I2M-TREFLE, UMR 5295, CNRS UB1 Arts et Métiers ParisTech,
Esplanade des Arts et Métiers 33405 Talence

Abstract. This work concerns the development of a non-contact calorimeter for two-phase flow characterization. The biphasic flow is performed under a droplet configuration inside millimetric tubings that are inserted into the isoperibolic chip. The main idea is to combine the Infrared Thermography and microfluidic tools to propose a suitable technique for accurate measurements. Microfluidics enables the use of small reaction volumes thus limiting any risk of dangerous reactions inside droplets; the Infrared tool enables to monitor the thermal signature of these flows with high accuracy. The results show that this tool is able to estimate the thermophysical properties of non-reactive flows. Also, it is possible to characterize chemical reactions in terms of enthalpy and kinetics. Finally the latter characterization was compared to conventional techniques to demonstrate the benefits and the precision of the tool.

5.1 Introduction

For reaction engineering purposes, the use of segmented flows, such as liquid liquid or liquid gas flows, in miniaturized devices has soared in recent years. Furthermore, recent advances have been made in the study of biphasic flows for the cooling systems of miniaturized electronic devices toward the improvement of micro-heat exchangers. The first thermal studies of liquid gas segmented flows used numerical and analytical approaches. Additionally, several experimental studies regarding the thermal effects and characterization of segmented liquid gas flows have been reported. These studies analyzed the influence of the length of the slugs to enhance the heat transfer in micro-channel heat sinks. In contrast, only one study on liquid-liquid thermal analysis has been reported. As a result, very few studies on the thermal analysis of liquid liquid flows, particularly with respect to the development of parameter estimation methods, have been reported in the literature. This workshop is a pragmatic attempt to implement thermal estimation methods for liquid liquid two-phase flows in miniaturized systems.
The main objective of this workshop in the field of thermal microfluidics is to develop new methods to determine the thermal properties; the enthalpy and kinetics of chemical reactions under biphasic flow. This work provides the first measurements of the temperature fields of liquid-liquid two-phase flows inside a millifluidic tubing-based isoperibolic chip and includes an estimation of the reaction heat flux and enthalpy. To achieve these estimations, our research has led to the development of:

- a non-contact droplet flow calorimeter,
- an experimental study related to the stability and periodicity of the flow,
- a quantitative thermal analysis,
- novel methods for identifying thermodynamic properties by using inverse processing methods,
- calorimeter validation for the characterization of a model reaction, and application to the characterization of two reactions,

In this workshop we will focus on the inverse processing methods for the estimation of thermophysical properties.

5.2 Key notions

5.2.1 Experimental setup

The millifluidic reactor shown in Figure 1(A) was designed using a bulk piece of brass for thermal control, whereas the flow set-up was realised inside of small-sized commercial perfluoroalkoxy (PFA) tubing and junctions (from Jasco). The bulk brass (Figure 1(A)) is thermally regulated (with a PID system) using a Peltier module with a temperature range from −5 to 70 °C for the accurate cooling and heating of the tubes inserted into the grooves of the bulk metal piece. Because PFA tubing is a good thermal insulator (k_{tube} = 0.10 $W.m^{-1}.K^{-1}$) and bulk brass is a good thermal conductor (kp = 380 $W.m^{-1}.K^{-1}$), the boundary condition of the external diameter of the tubing is assumed to work at the imposed temperature (i.e. isoperibolic). A heat sink paste was added between the tube and the brass plate. Consequently, the temperature inside the chemical reactor results from the heat transfer coefficient between the imposed temperature of the bulk brass and the inner diameter of the tube. Inside the tubing, the biphasic flow is delivered by a high-precision syringe pump (NEMESYS from Cetoni), where the oil (also called continuous phase) and droplets are generated by the injection of both fluids at different ratios. This allows for control of the hydrodynamic parameters, which include the total flow rate (i.e. the droplet velocity), the droplet size and the ratio between the oil and droplets. At the inlet of the tube schematic (Figure 1(B)), droplet generation is carried out using smaller tubes to deliver the reactants. The dimensions of the PFA tubing are 3.17 mm for the outer diameter and 1.6 mm for the inner diameter. The tubes used to supply the reactants have an outer diameter of 500 µm and an inner diameter of 350 µm. An infrared CEDIP camera (model JADE MWIR J550) is used for the temperature field measurements (Figure 1(C)). The IR sensor is a 240 × 320 pixel InSb focal plane array optimised for wavelengths ranging from 2 to 5.2 µm and a pitch of 30 µm. The IR objective lens is a 25 mm MWIR. With this objective, the spatial resolution of the temperature measured by each pixel of the sensor is approximately 250 µm in the object plane.

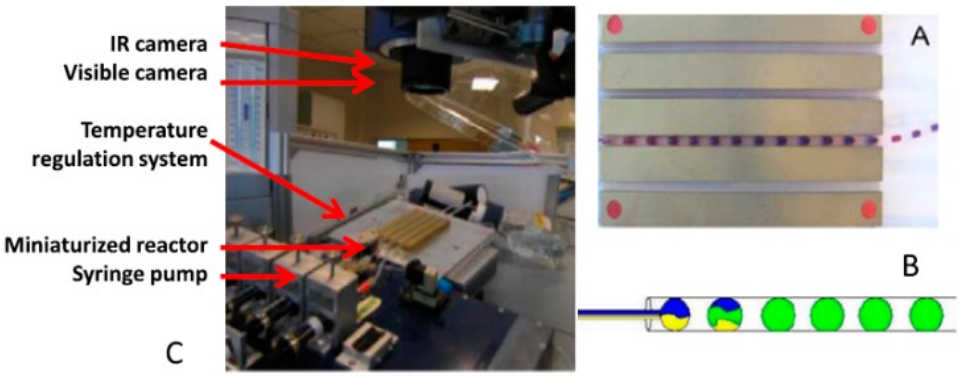

Figure 1: Scheme of the experiment

5.2.2 Modeling of the system

In Figure 2, different temperature fields are reported to demonstrate that the spatial evolution of the temperature is periodic. In this validation, the initial values of the temperatures of both the water and oil phases are equal to room temperature (20 °C) and the bulk brass, imposed at 30 °C, but are expressed on DL units. The thermal phenomena can be managed according to different orders. The observation of the IR raw temperature profile in Figure 2(A) demonstrates that the signal is composed of a continuous contribution (of order 1, see Figure 2(B)) and a fluctuating contribution (of order 2, see Figure 2(C)) according to the following expression:

$$T(z,t) = \overline{T}(z) + \widetilde{T}(z,t) \tag{5.1}$$

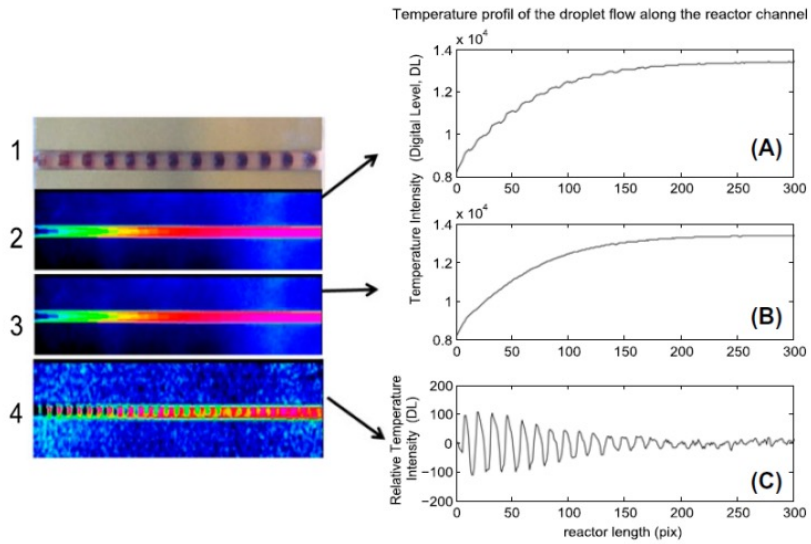

Figure 2 : Schematic of the thermal phenomena at different orders: (1) Visible image of the droplet flow at time t. (2) Infrared images of the temperature field measured at time t. (3) Averaged field over N periods. (4) Field of the fluctuating component. Right side: (A) Temperature profile along the channel at time t $T(z,t_i)$ from image 2, (B) temperature profile along the channel, where the temperature field is averaged over N periods $\overline{T}(z)$, (C) fluctuating profile along the channel $\widetilde{T}(z,t)$, obtained when signal B is subtracted from the field on signal A.

The fluctuating component highlights the presence of the biphasic flow, as shown in Figure 2(C), but represents less than 2% of the average signal of the continuous flow ($\overline{T}(z)$, Figure 2(B)). The continuous component (CC) resulting from the average value over N periods of each pixel of the channel is a function of the volume ratio of each phase. This is similar to achieving an overall space average in the local coordinate of the droplet–oil space. The different orders of the thermal behaviour of the biphasic flow are highlighted in Figure 2. At the end of the channel, where the imposed temperature is reached, the phases of the droplets and the oil cannot be distinguished. Finally, from this validation, we can assume from a thermal point of view that a model of two diffusive media in Lagrangian space is sufficient to represent the thermal behaviour of such a system. From an experimental point of view, the periodicity of the flow could be considered as an advantage with respect to signal averaging to significantly increase the signal-to-noise ratio.

The first-order thermal behaviour, also called the CC, is introduced. From an analytical point of view, and due to the periodicity of the flow, this CC can be expressed as a spatial weighted averaged, performed as function of time between the two plugs (the oil and the droplet):

$$\overline{T}_{CC}(t) = \frac{L_G \int_{z=0}^{L_G} T_G(z,t)\,dz + L_H \int_{z=L_G}^{L_T=L_G+L_H} T_H(z,t)\,dz}{L_T} \tag{5.2}$$

According to Equation (2), the weighted average profiles from the second-order thermal behaviour can be represented by a CC. Here, the idea is to exhibit how this CC (resulting from the weighted averaged Equation (2)) can be represented by an equivalent homogeneous medium expressed by a mixing law function of the volume fraction and the thermal property ratio of each phase. More precisely, in this approximation, only the parietal exchanges between this equivalent homogenous medium and the bulk are taken into account. From this last assumption, a one-temperature (1T) thin body equivalent homogenous medium model can be expressed as follows:

$$\frac{d\overline{T}_{CC}(z)}{dz} = \Phi(z) - H\left(\overline{T}_{CC}(z) - T_p\right)$$
$$avec : \Phi(z) = \frac{\phi(z)}{\left(\rho C_p V\right)^* U},\quad H = \frac{h_p S_L}{\left(\rho C_p V\right)^* U},\quad \left(\rho C_p V\right)^* = \left(\rho_G C_{pG} L_G + \rho_H C_{pH} L_H\right) S, \tag{5.3}$$

Where $\overline{T}_{CC}(z)$ (K), is the temperature of the coninuous component, ρ* (kg.m^{-3}), mass density of the homogeneous equivalent media, C_p* (J.kg^{-1}.K^{-1}) is the specific heat of the homogeneous equivalent media, V* (m^3) the volume of the homogeneous equivalent media, U (m.s^{-1}) the mean velocity of the flow, $\phi(z)$ (W) the heat source, h_p (W.m^{-2}.K^{-1}) is the parietal heat exchange coefficient between the tubing and the isoperibolic boundary, T_p (K) the parietal temperature, L (m) length of the slug, S (m²) section, S_L (m²) heat exchange area and, G or H index for water or oil.

The characteristic coefficient H can also be expressed as:

$$H = \frac{h_p S_L}{\left(\rho C_p V\right)^* U} = \frac{4 h_p L_T}{\rho_H C_{pH} L_H (1 + K\alpha)} \tag{5.4}$$
$$avec :\ K = \frac{\rho_G C_{pG}}{\rho_H C_{pH}},\quad \alpha = \frac{L_G}{L_H}$$

5.3 Workshop applications

5.3.1 Estimation of thermophysical properties

In this validation section, only an example of the experimental data fitted with the analytical solution (Equation (3)) based on the inverse method (Equation (5)) is represented in Figure 3.

$$\begin{bmatrix} T_{CC}(z_1) \\ \vdots \\ T_{CC}(z_N) \end{bmatrix} = \begin{bmatrix} 1 & \int_0^{z_1} T_{CC}(z)\,dz & z_1 \\ \vdots & \vdots & \vdots \\ 1 & \int_0^{z_N} T_{CC}(z)\,dz & z_N \end{bmatrix} \begin{bmatrix} T_{CC}(z_1) \\ H \\ HTp \end{bmatrix} \tag{5.5}$$

This example was investigated for a combination of pure water and fluorinated oil at a given total flow rate Q_T = 20 mL.h^{-1} and for R = 0.5–9. In this case, the initial values of the temperatures of both the water and oil phases are equal to room temperature (20 °C) and the bulk brass, imposed at 30 °C. The temperature profile of both the water and oil phases in coflow and for the same total flow rate are also measured. In Figure 15, the experimental temperature profiles of the droplet flow and the temperature profiles for both the water and oil alone in coflow at the same total flow are also plotted. When steady state is reached, a sequence of IR images is taken. Image processing is applied to extract the temperature intensity profiles (DL).

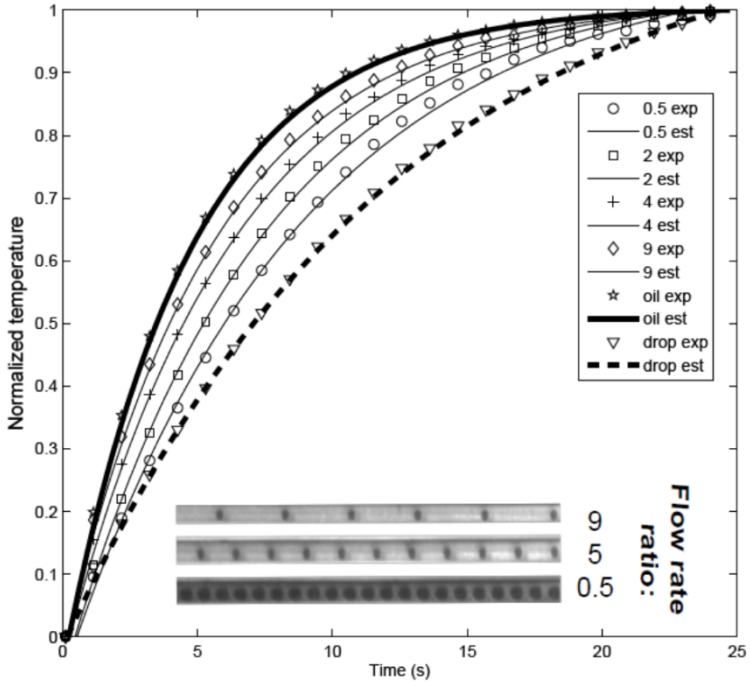

Figure 3: CC profile for a given total flow (Q_T) at different water-oil flow rate ratios. In the legend, the label *exp* concerns the experimental data, while the label *est* concerns the analytical estimations

Figure 3 shows that the measured CC temperature profiles are functions of the flow rate ratio between the droplet and the oil. When the volume fraction of the water droplets is higher (at R = 0.5), the average behavior of the system is similar to that of pure water. In contrast, when the volume fraction of the oil increases (at R = 9), the behavior of the CC is similar to that of pure oil. Moreover, in Figure 3, the profiles for the single flows estimated by Equation (3) are also represented. All of these analytical profiles are represented by solid lines, which are fit with good agreement to the experimental measurements. It should be noted that in Figure 3, the space and the shape of the droplets are significantly modified when R is modified. From a thermal point of view, this affects the heat transfer, and especially the heat exchange surface, between the fluids and the bulk. Nevertheless, the global thermal behavior released is bounded by that of the water and oil.

The H coefficient represents the inverse of either the characteristic time or length due the convective effects (m^{-1}). In Figure 4, the inverse of the estimated H is illustrated as a function of u, where $L_{DG}=L_H$. Figure 4 shows that the inverse of the characteristic coefficients decreases as the oil volume fraction increases (R = 9). The values for the pure water (represented at the abscissa as 0) and the values for the pure oil (represented at the abscissa as 1) are reported. For all of the experimental sets (Figure 4), the inverse of the characteristic coefficient tends to decrease with decreasing total flow.

In Figure 4, the effective heat exchange coefficients coming from Equation (5) are represented according to the following formulation:

$$\frac{1}{H} = \frac{1-K}{K_0}\left(\frac{1}{1+\alpha}\right) + \frac{K}{K_0} = au + b \qquad (5.6)$$

$$avec: \quad K_0 = \frac{\rho_H C_{pH} dU}{4h_P}, \quad K = \frac{\rho_G C_{pG}}{\rho_H C_{pH}}, \quad \alpha = \frac{L_G}{L_H}$$

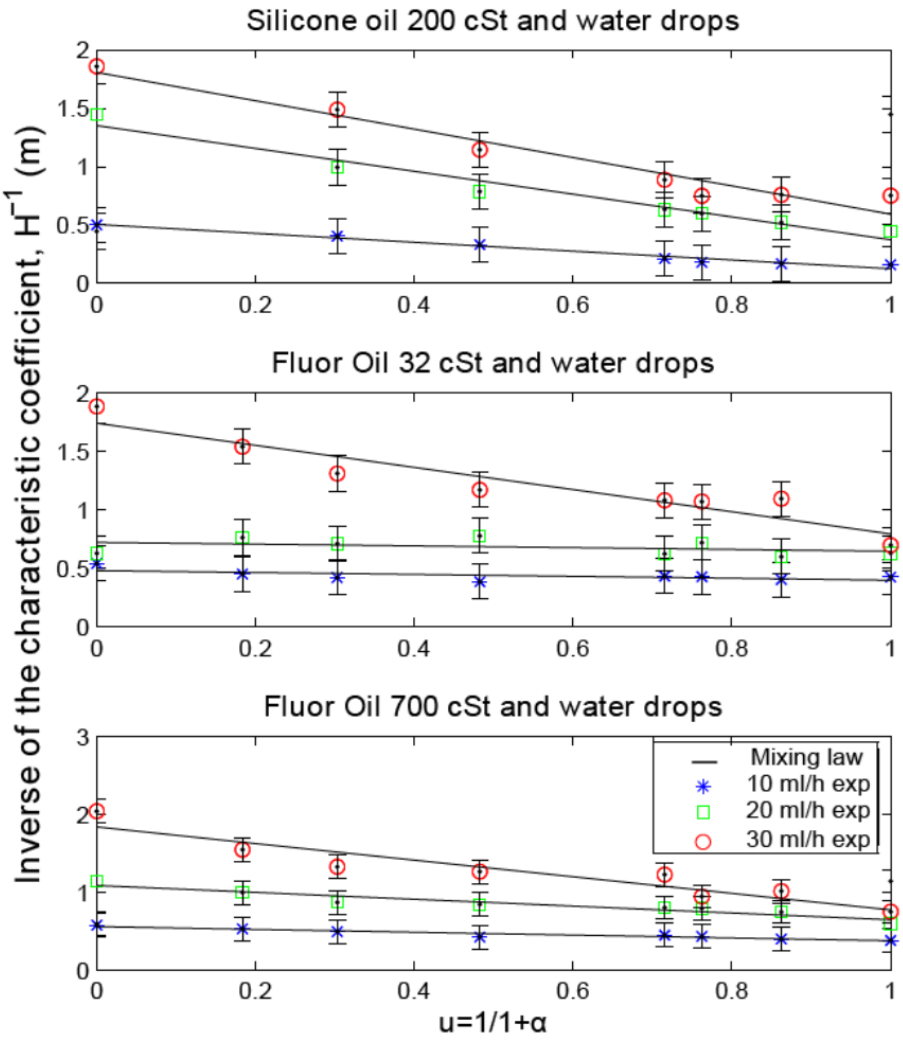

Figure 4: The inverse of the experimental H coefficients for several total flow rates and ratios R. From top to bottom. The first graph concerns the experimental set using silicone oil (250 cSt 25 °C) as the continuous phase. The second graph concerns the experimental set, using fluorinated oil (32 cSt 25 °C) as the continuous phase. The third graph concerns the experimental set, using fluorinated oil (700 cSt 25 °C) as the continuous phase. Pure water (abscissa 0) and oil (abscissa 1) are plotted at the edges.

From Equation (6), and by assuming that a ¼ L_G=L_HO is well known, the ratio K of Equation (6) can be estimated. by assuming that the thermal properties of the pure water are known and taken equal to be 4.18 × 10^6 (J.m^{-3}.K^{-1}), the properties of the several types of oils are estimated and compared with that given by the supplier and reported in table 1.

Oil type	K	Data from the supplier ρC_p ($J\,m^{-3}\,K^{-1}$)	K	Estimation ρC_p ($J\,m^{-3}\,K^{-1}$)	Absolute error (%)
Silicone oil 200 cSt	3.31	1.2628×10^6	3.20	1.3062×10^6	3
Fluorinated oil 32 cSt	2.23	1.8744×10^6	2.14	1.9533×10^6	4
Fluorinated oil 700 cSt	2.11	1.9810×10^6	2.14	1.9624×10^6	1

Notes: K is the ratio between the properties of both media, which is estimated and compared with the data given by the supplier. Because the droplet phase was fixed as a known (water), it is possible to estimate the properties of the oil phase.

Table 1 Results for the estimation of thermophysical properties

The absolute error is also given in Table 1, where it should be noted that the absolute error is found to be lower than 5%. Therefore, we are able to deduce the oil phase properties (ρC_p oil) from the estimated K, when the water properties have been fixed as known.

5.3.2 Estimation of kinetic and enthalpy of chemical reaction

The W coefficient represents the parietal heat losses due to the isoperibolic condition imposed by the brass bulk. This final calibration allows us to link the heat source dissipated inside the tubing with the temperature measured at its surface. An electrical conductive tin wire was introduced inside the tubing channel for this measurement. The temperature was measured in the arbitrary DL unit, and after calibration it is possible to relate the released energy to the digital intensity (these results are omitted here, but see [1,2] for more details). The correlation method was applied for the simultaneous estimations of the heat source and characteristic time due to the convective effects [3]. The enthalpy of the reaction (ΔH, unit: $kJ.mol^{-1}$), which acts as the heat source, requires a difficult estimation because in such cases the source term evolution is correlated with heat losses. Therefore, an acid-base chemical reaction with a well-known enthalpy was performed in this study. The estimated spatial or temporal distributions of the heat source do not correspond to the kinetics of the reaction, but rather more to a gradual mixing of the chemical products due to mass diffusion. The average temperature profiles (continuous contribution) of the chemical reaction for different flow rate ratios (R), described according to Eq. (3), are illustrated in Fig. 5. The temperature profile intensity (T, unit: DL) of the acid-base reaction tends to decrease as R is increased. Indeed, when the droplet-oil ratio is weak (e.g., R = 0.5) the relaxation time is higher and proportional to a higher molar flow. As the ratio increases (until R = 10) the molar flow decreases and the biphasic flow reaches the temperature imposed by the isoperibolic chip more quickly. It is important to note that the temperature profiles for the oil-droplet ratios of R = 8 and 10 are almost the same because the volume of the droplet is almost the same as well.

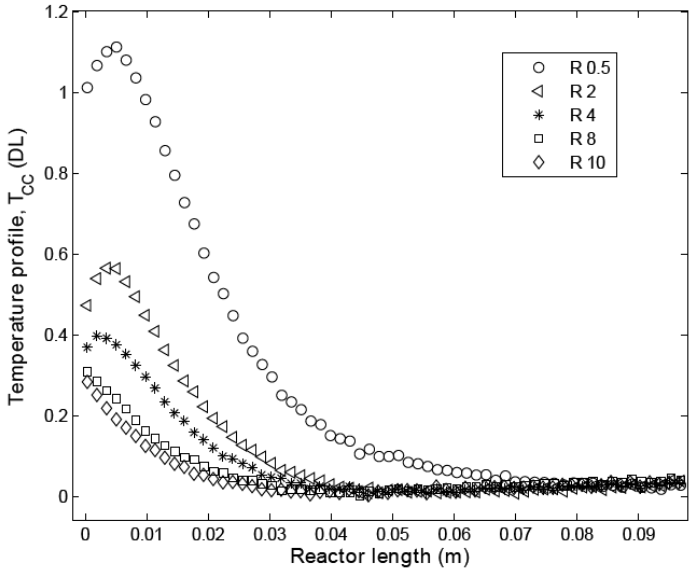

Figure 5: Measured temperature for an acid-base (C = 0.5 M) chemical reaction with a total flow rate of 10 ml.h^{-1} with IKV32 oil at room temperature as function of the flow rate ratio R.

From these measured temperatures an inverse processing method based on nodal approach by using correlation is implemented. The correlation method is applied for the simultaneous estimation of the heat source and the heat losses. The inverse process depicted here is an alternative method to the Gauss Markov estimation. When a heat source is present in equation 3, the difficulty that develops in the estimation resides in the evolution of the source term, which is correlated with the heat losses. To remove the heat loss information, it is important to detect the times during which only the heat source or the heat losses can be estimated. Our approach to solving this problem is to find a statistical estimator that can clearly detect the period at which the heat source is on and/or the heat losses are occurring. To detect this zone, the coefficient of correlation must be considered:

$$\rho^{Fz} = \frac{\sum_{Fz} \overline{T}_{CC}{}^{k} \frac{d\overline{T}_{CC}{}^{k}}{dz}}{\sqrt{\sum_{Fz} \overline{T}_{CC}{}^{k2}} \sqrt{\sum_{Fz} \frac{d\overline{T}_{CC}{}^{k}}{dz}^{2}}} \tag{5.7}$$

where $\overline{T}_{CC}$ is the mean temperature of the thin layer, $\frac{d\overline{T}_{CC}{}^{k}}{dz}$ is the temporal derivative of the average temperature of the thin layer, and Fz is a spatial window of length Fz = [k : k + lz], with k as the space step and lz as the length of spatial window. The correlation coefficient represents the normalized measure of the strength of the linear relationship between two variables equation 8. In our case, and according to equation 3, the mean surface temperature of the thin layer and its time derivative are the two variables of this linear relationship, expressed as follows:

$$\begin{aligned} &Y = aX + b \\ &with: Y = \frac{d\overline{T}_{CC}(z)}{dz},\ X = \overline{T}_{CC}(z) - T_p, a = -H \ and \ b = \Phi(z) \end{aligned} \tag{5.8}$$

the heat losses can be calculated with the formula:

$$H(z) = \rho^{Fz} \frac{\sum_{Fz} \overline{T}_{CC}^{\,k} \frac{d\overline{T}_{CC}^{\,k}}{dz}}{\sqrt{\sum_{Fz} \overline{T}_{CC}^{\,k2}}} \tag{5.9}$$

To perform an accurate estimation of the heat source (reaction enthalpy), the heat losses are estimated when the chemical reaction is finished (the heat source is off), based on the correlation methodology. In figure 6.A, the correlation as a function of time is shown, hence it can be observed that when the heat source is on (i.e., the chemical reaction is taking place), the correlation is equal to -1. Then, when the chemical reaction is finished, the correlation values are equal +1. From the moment at which the correlation values become positive, the heat losses are estimated. Figure 6 shows the H (m^{-1}) characteristic coefficient for each flow rate ratio R. As expected by the analytical validation, it becomes possible to experimentally verify that the H characteristic coefficient tends to stabilize after R=2, tending to a constant value.

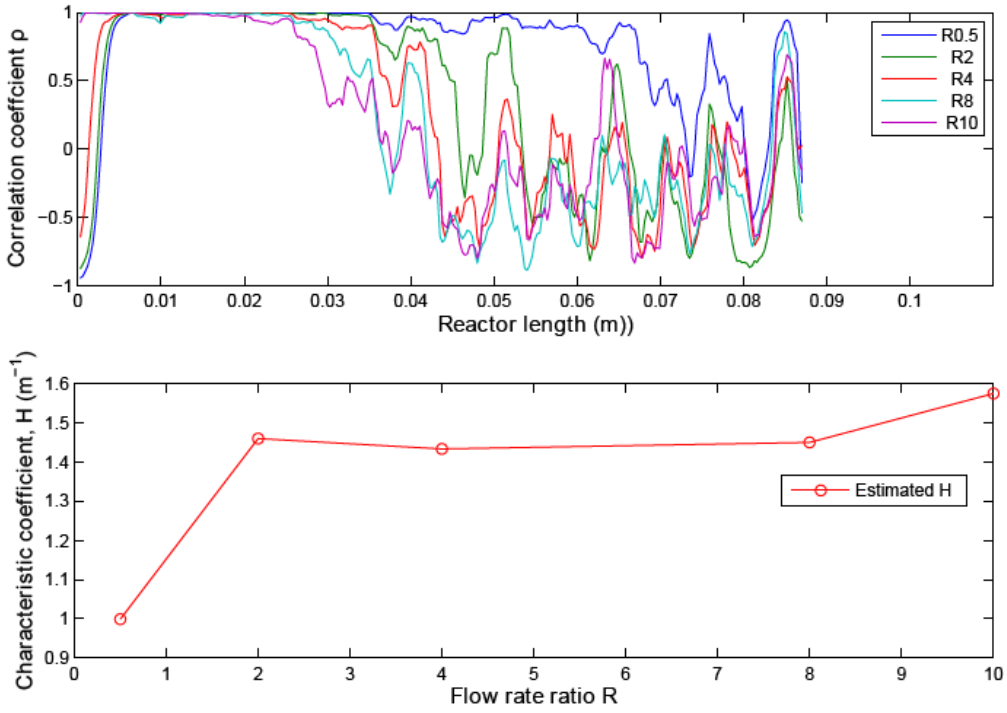

Figure 6: a) Coefficients de corrélations obtenues à partir de l'équation 5.6 lors d'une réaction acide-base pour différents rapports R et b) coefficients H estimés.

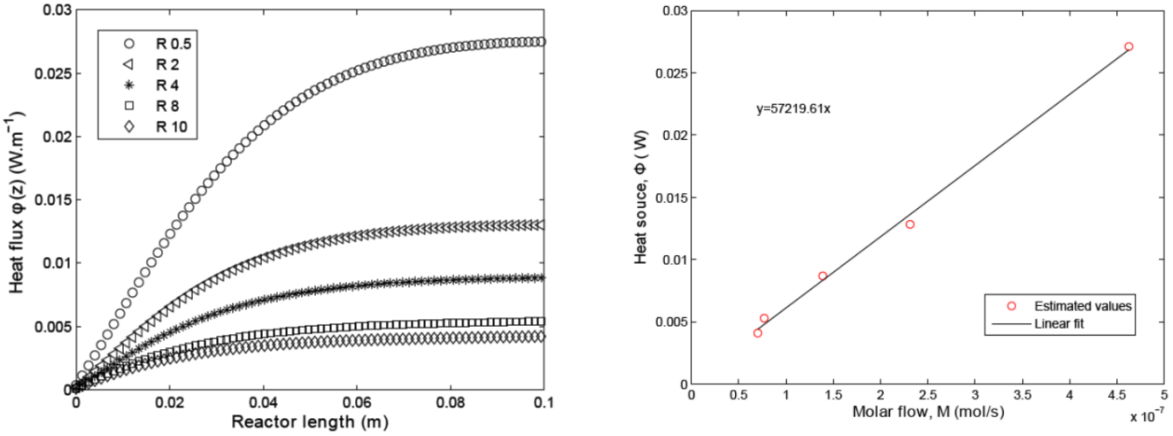

Figure 7: a), Heat source (unit: J) of the acid-base chemical reaction along the channel during the residence time. (b) Dissipated energy by the acid-base reaction at a total flow of 10 mL.h-1 for different droplet-oil flow ratios as a function of the injected reactants M

To avoid convective effects, it is important to pinpoint the time in which the heat source or the convective effects are estimable. From the knowledge of the exact zone where the heat source is off, it becomes possible to estimate the H coefficient as function of time. Alternatively, when the heat source is on, it is possible to estimate the heat source by applying Eq. (10).

$$\int_{z=0}^{L}\Phi(z)dz=\overline{T}_{CC}(z)+H\int_{z=0}^{L}\overline{T}_{CC}(z)dz-T_p(1+Hz)$$
$$avec:\Phi(z)=\frac{\phi(z)}{(\rho C_pV)^*U},\quad H=\frac{h_pS_L}{(\rho C_pV)^*U},\quad (\rho C_pL)^*=(\rho_GC_{pG}L_G+\rho_HC_{pH}L_H) \qquad (5.10)$$

In Eq. (10), Q is the integrated heat source over time (unit: J), M represents the injected concentration (unit: mol), C0 is the initial concentration of the limiting reactant (unit: mol.L^{-1}), Q_{lim} is the limiting reactive flow (unit: L.s^{-1}), and t_{res} is the residence time (unit: s). In this equation the factor of 1/2 is present because the reactant flows and the initial concentrations are the same. The temperatures profiles shown in Fig. 5 are processed using to obtain the heat source. The obtained heat source is subsequently integrated over time by applying Eq. (10), the results of which are displayed in Fig. 7A. Therefore, the energy dissipated by the reaction is characteristic of the nature of the species involved. Fig. 7A shows that the intensity of the dissipated heat source tends to decrease as the droplet-oil ratio is increased, which occurs because the molar flow of the reagents also decreases. Additionally, once the maximum heat from the source has been dissipated, the source remains constant over the channel. The plateau is not reached at the same time for all values of the oil-droplet ratio, which may be an indication of the mixing time. To make an accurate estimation of the enthalpy, the reaction has to be complete (fully mixed) because the integration of the heat source when the conversion is completed inside the channel provides direct access to the reaction enthalpy. The estimation of the enthalpy is performed by plotting the value of the plateau of the integrated heat source versus the concentration of the injected reactants. Fig. 7B shows the integrated heat source as a function of the molar flow rate. From this data, the enthalpy of reaction (mixing in this case) can be estimated from a linear regression analysis, the slope of which represents the estimated enthalpy. The obtained value is 57.22 kJ.mol^{-1} [4],which is in good agreement (less than 2% error) with the reported literature value of 56 kJ.mol^{-1} [5]. The uncertainties obtained from repeated measurements are

acceptable and the experimental repeatability for the enthalpy estimation is approximately 94%, indicating that the estimation is accurate.

5.4 Conclusion

In this work, we have demonstrated that the millifluidic device is a convenient and powerful tool for the development of a novel non-intrusive calorimetry for biphasic flow. Even if the complete thermal problem is very complex, due to the periodicity of the flow and the dimension of the system an equivalent tin body model based on the continuous component of the flow is enough to thermally represent the problem.
The conclusions of this work showed that there is no obstacle to estimate both thermal properties as well as the heat source in such biphasic flows. Additionally, this technique could be used to characterize other original fluids inside of droplets like nanofluids.

5.5 References

[1] C. Hany, C. Pradere, J. Toutain, J. Batsale, A millifluidic calorimeter with infrared thermography for the measurement of chemical reaction enthalpy and kinetics,
QIRT J. 5 (2) (2008) 211–219.
[2] M. Romano, C. Pradere, J. Toutain, C. Hany, J.C. Batsale, Quantitative thermal analysis of heat transfer in liquid–liquid biphasic millifluidic droplet flows, QIRT J. (2014) 1–27.
[3] C. Ravey, C. Pradere, J.C. Batsale, Heat transfer and correlation mapping for the estimation of thermophysical properties in microfluidic devices, ASME (2010).[4] M. Romano, C. Pradere, J. Toutain, J.C. Batsale,Quantitative kinetics and enthalpy measurements of biphasic underflow chemical reactions using InfraRed Thermography. ETFS (2014).
[5] D.R. Lidie (Ed.), Handbook of Chemistry and Physics, 72 ed., CRC Press, Ohio, 1992.